Inorganic Chemistry

Article

pubs.acs.org/IC

Photoluminescence Switching with Changes in the Coordination Number and Coordinating Volatile Organic Compounds in Tetracyanidonitridorhenium(V) and -technetium(V) Complexes

Hayato Ikeda,[†] Takashi Yoshimura,*[,†,‡] Akitaka Ito,[§] Eri Sakuda,[§,⊥] Noboru Kitamura,[§,⊥] Tsutomu Takayama,[∥] Tsutomu Sekine,[#] and Atsushi Shinohara[†]

[†]Department of Chemistry, Graduate School of Science, Osaka University, Toyonaka 560-0043, Japan

[‡]Radioisotope Research Center, Osaka University, Suita 565-0871, Japan

[§]Department of Chemistry, Faculty of Science, Hokkaido University, Sapporo 060-0810, Japan

[⊥]Department of Chemical Sciences and Engineering, Graduate School of Chemical Sciences and Engineering, Hokkaido University, Sapporo 060-0810, Japan

[∥]Department of Chemistry, Daido University, Nagoya 457-8530, Japan

[#]Center for the Advancement of Higher Education, Tohoku University, Sendai 980-8576, Japan

Supporting Information

ABSTRACT: Six-coordinate distorted octahedral tetracyanidonitridorhenium(V) and -technetium(V) complexes with a volatile organic compound (VOC) coordinating at the trans position of a nitrido ligand, $(PPh_4)_2[MN(CN)_4L]$ (M = Re, L = MeOH, EtOH, acetone, or MeCN; M = Tc, L = MeOH), and five-coordinate square-pyramidal tetracyanidonitrido complexes without an axial ligand, $(PPh_4)_2[MN(CN)_4]$ (M = Re or Tc), were synthesized and characterized. Single-crystal X-ray structural analysis was carried out for $(PPh_4)_2[MN(CN)_4L]$ (M = Re, L = MeOH, EtOH, or acetone; M = Tc, L = MeOH) and $(PPh_4)_2[ReN(CN)_4]$. All complexes studied showed photoluminescence in the solid state at room temperature. Reversible luminescence switching between six- and five-coordinate rhenium(V) complexes and between the relevant six-coordinate rhenium(V) complexes except that between the MeCN and acetone complexes was achieved by exposing them to VOC vapor in the solid state at room temperature. Luminescence changes were observed from the five-coordinate technetium(V) complexes in a MeOH vapor atmosphere in the solid state. In contrast, no vapochromic luminescence was observed from the five- and six-coordinate complexes in an acetone vapor atmosphere.

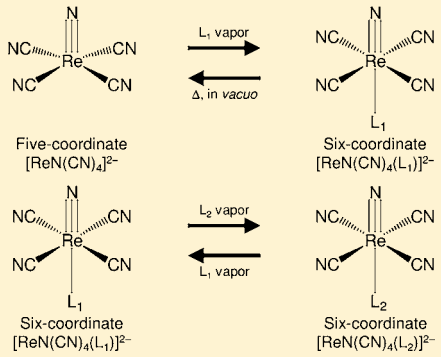

INTRODUCTION

Among the group 7 metal ions, several types of rhenium complexes show photoluminescence at room temperature, with representative examples being rhenium(I) polypyridyl, $[Re\{1,2\text{-bis(dialkylphosphinoethane)}\}_3]^{2+}$, dioxorhenium(V), nitridorhenium(V), quadruply bonded Re^{III}_2, and octahedral Re^{III}_6 complexes.[1−4] A very small number of technetium complexes have been reported to show photoluminescence: technetium(I) bipyridyl, $[Tc\{1,2\text{-bis-(dimethylphosphinoethane)}\}_3]^{2+}$, dioxotechnetium(V), and quadruply bonded Tc^{III}_2 complexes.[5] It is known that some metal complexes show reversible vapochromic luminescence in the solid state through changes in the metal−metal interaction,[6] coordination geometry,[6r,t,7] intermolecular interaction,[8] protonation on the ligand,[9] and coordination of volatile organic compounds (VOCs).[6r,10] In coordination compounds, molecular sensing can be done based on the color change of a complex through changes in the coordination environments and/or direct interaction of the metal ion with a molecule to be sensed. In contrast, molecular sensing based on vapochromic luminescence through a ligand substitution reaction and the coordination number of a metal ion in the solid state has rarely been reported.[6r,10]

It is known that nitridorhenium and -technetium complexes exist either as six-coordinate distorted octahedral or five-coordinate square-pyramidal structures.[11] Among these complexes, the nitridorhenium(V) complexes with a six- or five-coordinate structure were reported to show photoluminescence.[3a−c,e−h,12] In the six-coordinate rhenium and technetium complexes, the bond between the metal ion and the axial ligand at the trans site of the nitrido ligand is very weak; the axial site is labile because of the trans influence and trans effect of the nitrido ligand.[11] In the nitridotechnetium complexes, $[TcNX_5]^{2-}$ and $[TcNX_4]^-$ (X = Cl or Br), it was reported that the nature of a coexisting countercation in solution

Received: October 17, 2011
Published: November 2, 2012

   dx.doi.org/10.1021/ic202243d | Inorg. Chem. 2012, 51, 12065−12074

Table 1. Crystallographic Data of the $(PPh_4)_2$[1-Re-MeOH], $(PPh_4)_2$[1′-Re], $(PPh_4)_2$[1-Re-EtOH], $(PPh_4)_2$[1-Re-acetone], and $(PPh_4)_2$[1-Tc-MeOH] Complexes

	$(PPh_4)_2$[1-Re-MeOH]	$(PPh_4)_2$[1′-Re]	$(PPh_4)_2$[1-Re-EtOH]	$(PPh_4)_2$[1-Re-acetone]	$(PPh_4)_2$[1-Tc-MeOH]
formula	$C_{56}H_{43}N_5O_4P_2Re$	$C_{55}H_{47}N_5OP_2Re$	$C_{58}H_{50}N_5O_3P_2Re$	$C_{55}H_{46}N_5OP_2Re$	$C_{55}H_{40}N_5O_4P_2Tc$
fw	1098.14	1042.13	1113.22	1041.16	996.55
space group	$P\bar{1}$	$P\bar{1}$	$P2_1/a$	$P1$	$P\bar{1}$
a/Å	13.8212(6)	10.7379(4)	20.2827(6)	9.003(3)	13.427(9)
b/Å	16.4961(8)	11.4894(3)	13.2627(4)	11.174(3)	14.00(1)
c/Å	13.4479(6)	20.7772(6)	21.7579(7)	13.030(5)	16.64(1)
α/deg	89.701(1)	79.2564(9)	--	64.77(1)	108.67(1)
β/deg	62.2420(9)	78.353(1)	115.2569(7)	81.19(1)	90.16(1)
γ/deg	72.218(1)	77.2196(9)	--	80.08(1)	119.296(6)
V/Å^3	2549.2(2)	2421.2(1)	5296.2(3)	1163(2)	2535(3)
Z	2	2	4	1	2
T/K	170.2	170.2	170.2	170.2	170.2
ρ_{calc}/g cm^{-3}	1.431	1.429	1.396	1.486	1.302
μ/mm^{-1}	2.497	2.621	2.404	2.727	0.394
R1[a]	0.0589	0.0378	0.0376	0.0487	0.0785
wR2[a]	0.1417	0.1087	0.0920	0.1251	0.2407
GOF	1.123	1.098	1.069	1.092	1.044

[a] $R1 = \sum||F_o| - |F_c||/\sum|F_c|$. $wR2 = [\sum w(F_o^2 - F_c^2)^2/\sum w(F_o^2)^2]^{1/2}$.

determined the geometry of the complex: either five- or six-coordinate geometry.[13] On the basis of these viewpoints, both nitridorhenium(V) and -technetium(V) complexes with VOCs are expected to show photoluminescence switching through changes in the ligand by a substitution reaction and in the coordination number of the metal ion in the solid state.

In the present paper, we report novel six-coordinate nitridorhenium(V) and -technetium(V) complexes with VOCs at the axial sites. Their five-coordinate square-pyramidal complexes without an axial ligand were also synthesized. The present study demonstrated for the first time that the nitridotechnetium(V) complex showed luminescence in the solid phase at room temperature. It is worth emphasizing that the spectroscopic and photophysical properties of the new complexes are significantly dependent on the presence or absence of the axial ligand and the nature of the VOC (MeOH, EtOH, acetone, or MeCN). Furthermore, we demonstrate for the first time interconversion between the six-coordinate rhenium(V) complexes, except between the MeCN and acetone complexes, through a solid-state substitution reaction upon exposure to VOC vapor, and between the five-/six-coordinate complexes by a solid-state ligand coordination/elimination reaction. These interconversion reactions in the solid state were confirmed by vapochromic luminescence, IR, and ^{1}H NMR spectral changes.

EXPERIMENTAL SECTION

Materials. All commercially available reagents were used as received. The isotope ^{99}Tc was used to synthesize all of the technetium complexes reported in this paper. ***Caution!*** *^{99}Tc is a low-energy β^- emitter (E_{max} = 290 keV) with a half-life of 2.11 × 10^5 y. $K_2[ReN(CN)_4]\cdot H_2O$ and $\{(n\text{-}C_4H_9)N\}[TcNCl_4]$ were prepared according to literature procedures.*[13a,14]

Preparation of the Complexes. $(PPh_4)_2$[ReN(CN)$_4$(MeOH)]·3MeOH ($(PPh_4)_2$[1-Re-MeOH]). $K_2[ReN(CN)_4]\cdot H_2O$ (750 mg, 1.87 mmol) was dissolved in 11 mL of water, and $(PPh_4)Cl$ (2.00 g, 5.34 mmol) in 2 mL of water was added to the solution. The yellow suspension that formed immediately was heated to give a yellow solution, and then the solution was cooled to room temperature. The yellow solid obtained by filtration was dissolved in 15 mL of MeOH, and 35 mL of Et_2O was layered on the solution. The solution was allowed to stand for several days, and the yellow crystals formed were filtered. Yield of $(PPh_4)_2$[1-Re-MeOH]: 1.87 g (90.1%). Anal. Calcd for $C_{53}H_{44}N_5OP_2Re\cdot 3CH_3OH$: C, 60.53; H, 5.08; N; 6.30. Found: C, 60.19; H, 4.90; N, 6.36. ^{1}H NMR in $CDCl_3$: δ 3.47 ($-CH_3$ of MeOH), 7.52−7.89 (40H, phenyl of PPh_4). UV−vis [λ/nm (ε/M^{-1} cm^{-1}) in MeOH]: 387 (190), 276 (6400), 269 (7600). UV−vis in the solid state: 387 nm. IR (KBr pellet)/cm^{-1}: 2135 ($\nu_{C\equiv N}$), 2119 ($\nu_{C\equiv N}$), 2105 ($\nu_{C\equiv N}$), 1084 ($\delta_{H-O-C\ (MeOH)}$), 1037 ($\nu_{C-O\ (MeOH)}$). Raman in the solid state: 2135 ($\nu_{C\equiv N}$), 2117 ($\nu_{C\equiv N}$), 2101 ($\nu_{C\equiv N}$), 1086 ($\delta_{H-O-C\ (MeOH)}$) cm^{-1}.

$(PPh_4)_2$[ReN(CN)$_4$] ($(PPh_4)_2$[1-Re]). $(PPh_4)_2$[1-Re-MeOH] (330 mg, 0.297 mmol) was left at 95 °C for 4 h in vacuo. Yield of $(PPh_4)_2$[1-Re]: 283 mg (97.0%). Anal. Calcd for $C_{52}H_{40}N_5P_2Re$: C, 63.53; H, 4.10; N; 7.12. Found: C, 63.17; H, 4.10; N, 7.12. UV−vis in the solid state: 464 (sh), 383 nm. IR (KBr pellet): 2127 ($\nu_{C\equiv N}$), 2101 ($\nu_{C\equiv N}$) cm^{-1}. Raman in the solid state: 2128 ($\nu_{C\equiv N}$), 2116 ($\nu_{C\equiv N}$), 2108 ($\nu_{C\equiv N}$), 2101 ($\nu_{C\equiv N}$) cm^{-1}.

$(PPh_4)_2$[ReN(CN)$_4$]·*i*-PrOH ($(PPh_4)_2$[1′-Re]). $(PPh_4)_2$[1-Re] (125 mg, 0.128 mmol) was dissolved in 25 mL of isopropyl alcohol (*i*-PrOH), and then 25 mL of Et_2O was layered on the solution. The solution was left for several days to form yellow crystals. Yield: 81.4 mg (61.2%). Anal. Calcd for $C_{52}H_{40}N_5P_2Re\cdot(CH_3)_2CHOH\cdot H_2O$: C, 62.25; H, 4.75; N; 6.60. Found: C, 62.29; H, 4.76; N, 6.52. ^{1}H NMR in $CDCl_3$: δ 1.21 (d, 6H, $-CH_3$), 4.03 (m, 1H, −CH−), 7.60−7.89 (40H, phenyl of PPh_4). UV−vis [λ/nm (ε/M^{-1} cm^{-1}) in $CHCl_3$]: 379 (200), 277 (8300), 270 (9800). UV−vis in the solid state: 384 nm. IR (KBr pellet): 2128 ($\nu_{C\equiv N}$), 2106 ($\nu_{C\equiv N}$) cm^{-1}. Raman in the solid state: 2130 ($\nu_{C\equiv N}$), 2116 ($\nu_{C\equiv N}$), 2106 ($\nu_{C\equiv N}$) cm^{-1}.

$(PPh_4)_2$[ReN(CN)$_4$(EtOH)]·2EtOH ($(PPh_4)_2$[1-Re-EtOH]). $(PPh_4)_2$[1-Re] (88.4 mg, 0.0899 mmol) was dissolved in 1 mL of EtOH and then layered with 8 mL of Et_2O. The solution was left for several days, and the yellow crystals formed were filtered. Yield: 82.3 mg (81.6%). Anal. Calcd for $C_{52}H_{40}N_5P_2Re\cdot 0.5C_2H_5OH\cdot 3H_2O$: C, 60.05; H, 4.66; N; 6.61. Found: C, 59.75; H, 4.59; N, 6.57. ^{1}H NMR in $CDCl_3$: δ 1.24 (t, 1.5H, $-CH_3$ of EtOH), 3.72 (m, 1H, $-CH_2-$ of EtOH), 7.60−7.90 (40H, phenyl of PPh_4). UV−vis [λ/nm (ε/M^{-1} cm^{-1}) in EtOH]: 391 (200), 276 (7500), 269 (8800). UV−vis in the solid state: 380 (sh) nm. IR (KBr pellet): 2128 ($\nu_{C\equiv N}$), 2104 ($\nu_{C\equiv N}$) cm^{-1}. Raman in the solid state: 2129 ($\nu_{C\equiv N}$), 2113 ($\nu_{C\equiv N}$), 2104 ($\nu_{C\equiv N}$), 2097 ($\nu_{C\equiv N}$) cm^{-1}.

$(PPh_4)_2$[ReN(CN)$_4$(acetone)] ($(PPh_4)_2$[1-Re-acetone]). $(PPh_4)_2$[1-Re] (47.3 mg, 0.0481 mmol) was dissolved in 20 mL of acetone and layered with 30 mL of Et_2O. The solution was left for

dx.doi.org/10.1021/ic202243d | Inorg. Chem. 2012, 51, 12065−12074

several days, and the yellow crystalline precipitate was filtered. Yield: 36.9 mg (73.6%). Anal. Calcd for $C_{55}H_{46}N_5OP_2Re$: C, 63.45; H, 4.45; N; 6.73. Found: C, 63.30; H, 4.42; N, 6.76. ^{1}H NMR in $CDCl_3$: δ 2.17 (s, 6H, $-CH_3$ of acetone), 7.61−7.90 (40H, phenyl of PPh_4). UV−vis [λ/nm (ε/M^{-1} cm^{-1}) in acetone]: 450 (sh, 80), 390 (180). UV−vis in the solid state: 397 nm. IR (KBr pellet): 2121 ($\nu_{C\equiv N}$), 2100 ($\nu_{C\equiv N}$), 1684 ($\nu_{C=O\ (acetone)}$) cm^{-1}. Raman in the solid state: 2122 ($\nu_{C\equiv N}$), 2106 ($\nu_{C\equiv N}$), 2097 ($\nu_{C\equiv N}$), 1684 ($\nu_{C=O\ (acetone)}$) cm^{-1}.

$(PPh_4)_2$[ReN(CN)$_4$(MeCN)] ($(PPh_4)_2$[1-Re-MeCN]). **$(PPh_4)_2$[1-Re]** (88.2 mg, 0.0897 mmol) was dissolved in 1 mL of MeCN and layered with 8 mL of Et_2O. The solution was left for several days, and the yellow crystals formed were filtered. Yield: 82.0 mg (89.3%). Anal. Calcd for $C_{54}H_{43}N_6P_2Re$: C, 63.33; H, 4.23; N; 8.21. Found: C, 63.04; H, 4.21; N, 8.24. ^{1}H NMR in $CDCl_3$: δ 2.00 (s, 3H, $-CH_3$ of MeCN), 7.61−7.90 (40H, phenyl of PPh_4). UV−vis [λ/nm (ε/M^{-1} cm^{-1}) in MeCN]: 397 (190), 276 (7000), 269 (8300). UV−vis in the solid state: 393 nm. IR (KBr pellet): 2281 ($\nu_{C\equiv N(MeCN)}$), 2251 ($\nu_{C\equiv N(MeCN)}$), 2123 ($\nu_{C\equiv N}$), 2102 ($\nu_{C\equiv N}$) cm^{-1}. Raman in the solid state: 2251 ($\nu_{C\equiv N(MeCN)}$), 2125 ($\nu_{C\equiv N}$), 2110 ($\nu_{C\equiv N}$), 2105 ($\nu_{C\equiv N}$), 2100 ($\nu_{C\equiv N}$) cm^{-1}.

$(PPh_4)_2$[TcN(CN)$_4$(MeOH)] ($(PPh_4)_2$[1-Tc-MeOH]). {(n-$C_4H_9)_4N$}[$TcNCl_4$] (72.2 mg, 0.145 mmol) was dissolved in 3 mL of CH_3CN, and KCN (326 mg, 5.00 mmol) dissolved in 1 mL of water was added to the solution. The mixture was stirred for several minutes, and then the solution was evaporated to dryness. The residue was dissolved in 2 mL of H_2O, and $(PPh_4)Cl$ (483 mg, 1.29 mmol) in 7 mL of water was added to the solution. The resulting colorless solid precipitate was removed by decantation. The aqueous layer was extracted with 5 mL of CH_2Cl_2, and the organic layer was evaporated to dryness. The residue was recrystallized from a MeOH/Et_2O mixture to give large yellow crystals. Yield: 67.6 mg (45%). UV−vis [λ/nm (ε/M^{-1} cm^{-1}) in MeOH]: 396 (140), 276 (7800), 269 (9200). UV−vis in the solid state: 408 nm. IR (KBr pellet): 2138 ($\nu_{C\equiv N}$), 2120 ($\nu_{C\equiv N}$), 2113 ($\nu_{C\equiv N}$), 1076 ($\delta_{H-O-C\ (MeOH)}$), 1038 ($\nu_{C-O\ (MeOH)}$) cm^{-1}.

$(PPh_4)_2$[TcN(CN)$_4$] ($(PPh_4)_2$[1-Tc]). **$(PPh_4)_2$[1-Tc-MeOH]** (65.3 mg, 0.0635 mmol) was left at 95 °C for 4 h in vacuo. Yield of **$(PPh_4)_2$[1-Tc]**: 48.1 mg (84%). UV−vis in the solid state: 400 nm. IR (KBr pellet): 2129 ($\nu_{C\equiv N}$), 2115 ($\nu_{C\equiv N}$) cm^{-1}.

X-ray Crystallography. The single-crystal X-ray data were collected at −103 °C on a Rigaku R-AXIS diffractometer with graphite-monochromated Mo Kα radiation. The crystal structures were solved by the Patterson method (*DIRDIF94*) or the direct method (*SIR92*). Atomic coordinates and thermal parameters of non-H atoms were calculated by a full-matrix least-squares method. The N(1) atom of $(PPh_4)_2$[ReN(CN)$_4$(acetone)] was refined isotropically. Calculations were performed using a *TEXSAN* software package.[15] Crystal data are summarized in Table 1.

Physical Measurements. ^{1}H NMR spectra were recorded on a Varian Mercury 300 MHz spectrometer. All peaks were referred to the proton signal of $Si(CH_3)_4$ at δ 0.00. UV−vis spectra in solution were recorded on a Jasco V-550 spectrophotometer. Solid-state reflectance UV−vis spectra were measured by a Jasco V-550 spectrophotometer equipped with an integration sphere, and a sample was placed between two silica glass plates. IR spectra were recorded on a Jasco FTIR-6100 or Perkin-Elmer 983G spectrophotometer. Raman spectra were measured by a Jasco NR-1800 laser Raman spectrophotometer with an excitation wavelength of 632.8 nm using a He−Ne laser as a light source. Elemental analysis was performed by the Analysis Center at Osaka University. Thermogravimetric and differential thermal analyses were conducted using a Seiko TG/DTA 200 instrument and temperature increase rates of 1 °C min^{-1}. Corrected emission spectra of the rhenium complexes were measured by using a multichannel photodetector (Hamamatsu Photonics PMA-11, excitation wavelength = 355 nm). The emission quantum yields were measured by an absolute emission quantum yield measurement system (Hamamatsu Photonics C9920-02) composed of an integrating sphere, a multichannel photodetector (Hamamatsu Photonics PMA-12), and a xenon lamp as an excitation light source (excitation wavelength = 400 nm). For emission lifetime measurements, a solid sample was placed between two nonfluorescent glass plates or in a glass cell under the given solvent vapor atmosphere. A pulsed Nd^{3+}:YAG laser (Lotis TII Ltd. LS-2137, 355 nm, fwhm ∼6 ns) was used as an excitation light source. The emission lifetime was measured by using a streak camera (Hamamatsu Photonics C4334). A liquid-N_2 cryostat (Oxford Instruments DN1704 optical Dewar and 3120 temperature controller) was used to control the sample temperature. For emission spectroscopy of the technetium complexes and studies on the vapochromic luminescence behavior of the rhenium and technetium complexes, the corrected emission spectra were recorded on a multichannel photodetector (Hamamatsu Photonics PMA-11) at 365 nm (±5 nm) excitation using a 100 W mercury−xenon lamp (HOYA-SCHOTT HLS 100UM) and an optical band-pass filter (Asahi Spectra).

RESULTS AND DISCUSSION

Synthesis and Characterization of the Complexes. The six-coordinate nitridorhenium(V) complex with a MeOH ligand, **$(PPh_4)_2$[1-Re-MeOH]**, was obtained by the metathesis reaction and isolation from the MeOH/Et_2O solution as described in the Experimental Section. The integrated proton signal intensity ratio of MeOH to $(PPh_4)^+$ observed for the ^{1}H NMR spectrum of **$(PPh_4)_2$[1-Re-MeOH]** was 4:2. This ratio was in good agreement with the result of the single-crystal X-ray analysis of the complex. When the crystals were left in air for 24 h at room temperature, the integrated proton signal intensity ratio of MeOH to $(PPh_4)^+$ became 0.33:2, indicating that both the coordinating axial MeOH ligand and three noncoordinating MeOH molecules in the crystal lattice gradually evaporated in air at room temperature. In fact, thermogravimetric measurements revealed that MeOH in the crystals including the coordinating MeOH ligands were removed in the range 25−70 °C at a temperature increase rate of 1 °C min^{-1}, as shown in the Supporting Information, Figure S1. MeOH in the crystals completely disappeared after the complex was heated at 95 °C in vacuo for 4 h, which was confirmed by ^{1}H NMR and IR spectra; the signals originating from MeOH disappeared after heating, demonstrating the formation of **$(PPh_4)_2$[1-Re]**. It is worth emphasizing that recrystallization of **$(PPh_4)_2$[1-Re]** from an *i*-PrOH/Et_2O solution affords the relevant five-coordinate square-pyramidal complex; the crystallized complex is abbreviated as **$(PPh_4)_2$[1′-Re]**. The ^{1}H NMR spectrum of **$(PPh_4)_2$[1-Re]** in $CDCl_3$ showed no MeOH signal, and the IR bands at ν_{C-O} 1037 and δ_{H-O-C} 1084 cm^{-1} ascribed to the MeOH molecules in **$(PPh_4)_2$[1-Re-MeOH]** disappeared in **$(PPh_4)_2$[1-Re]** (Supporting Information, Figure S2). Moreover, the IR frequencies of $\nu_{C\equiv N}$ observed for both **$(PPh_4)_2$[1-Re]** and **$(PPh_4)_2$[1′-Re]** in the solid state were very similar to each other. Therefore, we conclude that **$(PPh_4)_2$[1-Re]** is best characterized as a five-coordinate square-pyramidal complex without an axial ligand.

$(PPh_4)_2$[1-Re-EtOH], **$(PPh_4)_2$[1-Re-acetone]**, and **$(PPh_4)_2$[1-Re-MeCN]** were obtained by the reactions of **$(PPh_4)_2$[1-Re]** with EtOH, acetone, and MeCN, respectively. When the **$(PPh_4)_2$[1-Re-acetone]** and **$(PPh_4)_2$[1-Re-MeCN]** crystals were left in air for several days at room temperature, the integrated proton intensity ratio of the solvent ligand (acetone or MeCN) to $(PPh_4)^+$ in each complex remained 1:2, as confirmed by ^{1}H NMR spectroscopy in $CDCl_3$. Thermogravimetric measurements at a temperature increase rate of 1 °C min^{-1} revealed that the three EtOH molecules in **$(PPh_4)_2$[1-Re-EtOH]** including coordinating EtOH per complex were eliminated from the crystal lattice in the range 25−70 °C (Supporting Information, Figure S3). In the case of the acetone- and MeCN-coordinating complexes, elimination of

dx.doi.org/10.1021/ic202243d | *Inorg. Chem.* 2012, 51, 12065−12074

Table 2. Selected Bond Distances (Å) and Angles (deg) of the $(PPh_4)_2$[1-Re-MeOH], $(PPh_4)_2$[1′-Re], $(PPh_4)_2$[1-Re-EtOH], $(PPh_4)_2$[1-Re-acetone], and $(PPh_4)_2$[1-Tc-MeOH] Complexes

	$(PPh_4)_2$[1-Re-MeOH]	$(PPh_4)_2$[1′-Re]	$(PPh_4)_2$[1-Re-EtOH]	$(PPh_4)_2$[1-Re-acetone]	$(PPh_4)_2$[1-Tc-MeOH]
M≡N	1.652(6)	1.626(4)	1.646(4)	1.61(1)	1.612(7)
M−C	2.098(6)−2.115(7), av. 2.11 (1)	2.096(4)−2.103(4), av. 2.100(9)	2.091(4)−2.114(3), av. 2.102(7)	2.11(1), av. 2.11(2)	2.078(6)−2.104(6), av. 2.09(1)
C≡N	1.15(1)−1.170(9), av. 1.16(1)	1.145(5)−1.146(7), av. 1.15(1)	1.145(5)−1.154(5), av. 1.15(1)	1.13(2)−1.17(1), av. 1.15(3)	1.140(9)−1.172(8), av. 1.16(2)
M−O	2.439(5)		2.503(3)	2.604(6)	2.462(6)
N≡M−C	97.7(3)−99.7(3), av. 98.7(6)	103.8(2)−106.3(2), av. 104.2(4)	98.9(2)−100.8(2), av. 99.9(3)	97.6(4)−101.0(4), av. 99.6(9)	97.7(3)−99.8(3), av. 98.8(6)
C−Re−C (trans)	160.8(3)−164.4(3), av .162.6(4)	149.5(2)−153.6(2), av. 151.6(3)	159.9(1)−160.2(2), av. 160.1(2)	160.1(4)−160.4(4), av. 160.3(6)	160.4(3)−164.3(3), av. 162.4(4)
C−Re−C (cis)	87.7(2)−90.0(2), av. 88.7(4)	84.7(2)−87.9(2), av. 86.6(4)	86.5(1)−89.5(1), av. 88.3(2)	84.7(4)−92.0(5), av. 88.4(9)	86.6(2)−90.2(2), av. 88.7(4)

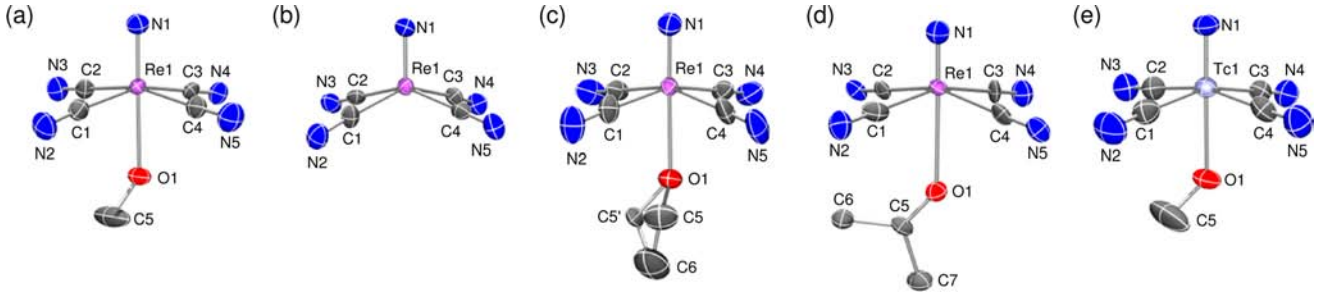

Figure 1. ORTEP drawings of the complex anions for $(PPh_4)_2$[1-Re-MeOH] (a), $(PPh_4)_2$[1′-Re] (b), $(PPh_4)_2$[1-Re-EtOH] (c), $(PPh_4)_2$[1-Re-acetone] (d), and $(PPh_4)_2$[1-Tc-MeOH] (e). H atoms are omitted for clarity. Thermal ellipsoids are shown at the 50% probability level.

the coordinating acetone and MeCN molecules was observed at a higher temperature compared with that of the MeOH molecule in $(PPh_4)_2$[1-Re-MeOH] (Supporting Information, Figures S4 and S5). The coordinating solvent molecules in all of the rhenium complexes were completely removed in vacuo at 95 °C for 4 h to recover $(PPh_4)_2$[1-Re]. Conversions between the six-coordinate MeOH, EtOH, acetone, and MeCN complexes and those between the six- and five-coordinate complexes were reversible, while the conversions between the six-coordinate MeCN and acetone complexes were irreversible, as described later. Although many square-pyramidal five-coordinate and octahedral six-coordinate d^2 metal complexes have been reported, $(PPh_4)_2$[1-Re-L] (L = MeOH, EtOH, acetone, or MeCN) and $(PPh_4)_2$[1-Re] are the first d^2 photoluminescent complexes showing reversible coordination environment switching, as described in later detail.

The nitridotechnetium(V) complex with an axial MeOH, $(PPh_4)_2$[1-Tc-MeOH], was prepared with a procedure similar to that used for $[TcN(CN)_4(H_2O)]^{2-}$, except with a slight modification for isolating the compound from a MeOH/Et_2O mixture.[16] $(PPh_4)_2$[1-Tc] was obtained by procedures analogous with those for the preparation of the rhenium complex. As seen in the IR spectrum of $(PPh_4)_2$[1-Tc] (Supporting Information, Figure S6), the ν_{C-O} and δ_{H-O-C} bands of MeOH at 1038 and 1076 cm^{-1} observed for $(PPh_4)_2$[1-Tc-MeOH] disappeared. This behavior was similar to that of the rhenium analogue. On the basis of these results, $(PPh_4)_2$[1-Tc] was characterized as a five-coordinate square-pyramidal complex. The reaction of $(PPh_4)_2$[1-Tc] with acetone in an acetone/Et_2O solution did not occur and gave $(PPh_4)_2$[1-Tc] in a high yield (90%).

Crystal Structures. The crystal structures of $(PPh_4)_2$[1-Re-MeOH], $(PPh_4)_2$[1′-Re], $(PPh_4)_2$[1-Re-EtOH], $(PPh_4)_2$[1-Re-acetone], and $(PPh_4)_2$[1-Tc-MeOH] were determined by single-crystal X-ray analysis. The selected bond distances/angles are summarized in Table 2. The crystal structures of these complexes are also shown in Figure 1. The complex anions of $(PPh_4)_2$[1-Re-MeOH], $(PPh_4)_2$[1-Re-EtOH], $(PPh_4)_2$[1-Re-acetone], and $(PPh_4)_2$[1-Tc-MeOH] have six-coordinate distorted octahedral structures. In each complex, one nitrido group is located at the axial site and a solvent molecule occupies the trans position to the nitrido group. The complex $[1'\text{-Re}]^{2-}$ possesses the five-coordinate square-pyramidal structure with one nitrido and four cyanido groups. The Re≡N bond distances [1.61(1)−1.652(6) Å] observed for both the five- and six-coordinate complexes were similar to one another. The M≡N bond distance was shorter in the technetium complex [1.612(7) Å] than the rhenium analogue [1.652(6) Å]. This trend is also found in axial-water-coordinating tetracyanidonitrido complexes, $[MN(CN)_4(H_2O)]^{2-}$ [M = Tc, Tc≡N = 1.596(10) Å; M = Re, Re≡N = 1.639(8)−1.657(2) Å].[16,17] The N≡Re−C angle [av. 104.2(4)°] in the five-coordinate complex is large compared with the six-coordinate complexes [av. 98.7(6)−99.9(3)°]. The C−Re−C (trans) angles in the five-coordinate complex [av. 151.6(3)°] are significantly smaller than those in the six-coordinate complexes [av. 160.1(2)−162.6(4)°]. These results may be due to the absence of an axial ligand. A similar tendency was reported for the tetracyanidonitridomanganese(V) complexes; the N≡Mn−C [av. 102.7(2)−102.8(2)°] and C−Mn−C (trans) angles [av. 154.4(2)−154.5(1)°] in the five-coordinate complex are larger and smaller than those in the six-coordinate complexes, $[MnN(CN)_4L]^{n-}$ (L = pyridine, 3- or 4-picoline, n = 2; L = CN or NCS, n = 3), respectively.[18] The M−C bond distances in both the rhenium and technetium complexes are very similar to each other. The bond distance between the metal ion and the O atom in the coordinating solvent molecule is significantly long because of the trans

dx.doi.org/10.1021/ic202243d | Inorg. Chem. 2012, 51, 12065−12074

Table 3. Spectroscopic and Photophysical Data in the Solid State at 296 and 77 K

	296 K			77 K	
	λ_{em}/nm (fwhm/cm^{-1})	Φ_{em}	τ_{em}/μs (% component)	λ_{em}/nm	τ_{em}/μs (% component)
$(PPh_4)_2$[**1-Re-MeOH**]	527 (3180)	0.13	0.41 (83), 2.2 (12), 11 (5)	496, 523, 552	77
$(PPh_4)_2$[**1-Re-EtOH**]	548 (3800)	<0.01	5.5 (58), 18 (42)	493, 520, 541, 551	4.9 (83), 55 (17)
$(PPh_4)_2$[**1-Re-acetone**]	533 (3240)	0.34	21	505, 531, 560	109
$(PPh_4)_2$[**1-Re-MeCN**]	545 (3300)	0.02	2.0	551	166
$(PPh_4)_2$[**1-Re**]	569, 720	<0.01	0.35 (61), 1.2 (35), 7.6 (4)	721	0.29 (52), 3.3 (17), 14 (31)
$(PPh_4)_2$[**1′-Re**]	689 (5200)	0.02	4.5	681	83
$(PPh_4)_2$[**1-Tc-MeOH**]	559 (3240)				
$(PPh_4)_2$[**1-Tc**]	528 (4040)				

influence of the nitrido ligand. The Tc−O distance [2.462(6) Å] in [**1-Tc-MeOH**]$^{2-}$ is longer than that of the isomorphic rhenium complex [2.439(5) Å]. It is noted that the Re−O bond distance is longer in the order MeOH [2.439(5) Å] < EtOH [2.503(3) Å] < acetone [2.604(6) Å]. The long M−O distance observed in the acetone-coordinating complex would be due to the steric hindrance between the methyl moiety of the acetone and cyanide ligands. This is supported by the fact that the more sterically hindered isopropyl alcohol does not coordinate at the axial site of the complex and hence produces a five-coordinate complex.

UV−Vis Spectra. The UV−vis spectra of the complexes in both solid and solution phases were studied at room temperature. The spectra of $(PPh_4)_2$[**1-Re-MeOH**], $(PPh_4)_2$[**1-Re-EtOH**], $(PPh_4)_2$[**1-Re-acetone**], $(PPh_4)_2$[**1-Re-MeCN**], $(PPh_4)_2$[**1-Re**], and $(PPh_4)_2$[**1′-Re**] are shown in the Supporting Information, Figures S7 −S11, respectively. The absorption bands of the six-coordinate complexes in neat solutions and in the solid states were observed in the wavelength (λ) region of 380−400 nm. The UV−vis reflectance spectra of $(PPh_4)_2$[**1-Re**] and $(PPh_4)_2$[**1′-Re**] in the solid states showed bands at 383 nm, a value similar to the maximum wavelength of $(PPh_4)_2$[**1-Re-MeOH**] in the solid state (λ_{max} = 387 nm). The absorption band can be ascribed to the $(d_{xy})^2 \rightarrow (d_{xy})^1(d_{\pi^*})^1$ ($d_{\pi^*} = d_{xz}, d_{yz}$) transition with $p_\pi(N^{3-})-d_\pi$ overlap. This electronic transition between the highest energy occupied molecular orbital (HOMO) and lowest energy unoccupied molecular orbital (LUMO) is well characterized in d^2 nitridorhenium complexes.[3c,e−g]

The UV−vis spectra of $(PPh_4)_2$[**1-Tc-MeOH**] and $(PPh_4)_2$[**1-Tc**] are shown in the Supporting Information, Figures S12 and S13, respectively. The spectral band shapes of $(PPh_4)_2$[**1-Tc-MeOH**] in both the solid state and MeOH are similar to those of the corresponding rhenium complex. The maximum wavelengths in MeOH (396 nm) and in the crystalline phase (408 nm) observed for $(PPh_4)_2$[**1-Tc-MeOH**] are slightly longer than the relevant value for the rhenium analogue (387 nm). This trend can also be seen in the λ_{max} values of $(PPh_4)_2$[**1-Tc**] (400 nm) and $(PPh_4)_2$[**1-Re**] (383 nm) in the solid state. These absorption bands of the technetium complexes could also be assigned to the $(d_{xy})^2 \rightarrow (d_{xy})^1(d_{\pi^*})^1$ transition.

Emission Spectroscopic and Photophysical Properties. All of the complexes showed photoluminescence in the solid state at room temperature. Table 3 summarizes the spectroscopic and photophysical data observed in the solid state at 296 and 77 K. To the best of our knowledge, these complexes are the first reported tetracyanidonitridorhenium(V) complexes showing photoluminescence. Figure 2 shows the emission spectra of the rhenium complexes in the crystalline

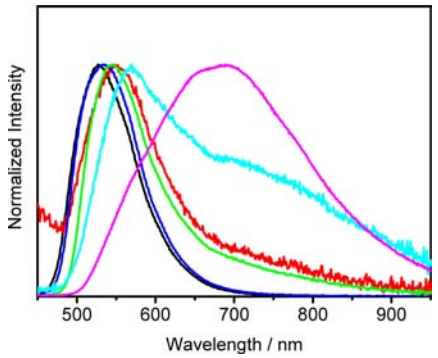

Figure 2. Emission spectra of $(PPh_4)_2$[**1-Re-MeOH**] (black), $(PPh_4)_2$[**1-Re-EtOH**] (red), $(PPh_4)_2$[**1-Re-acetone**] (blue), $(PPh_4)_2$[**1-Re-MeCN**] (lime green), $(PPh_4)_2$[**1-Re**] (cyan), and $(PPh_4)_2$[**1′-Re**] (magenta) in the solid state at 296 K.

phases at 296 K. The emission maximum (λ_{em}) was observed at longer wavelength in the order $(PPh_4)_2$[**1-Re-MeOH**] (527 nm) < $(PPh_4)_2$[**1-Re-acetone**] (533 nm) < $(PPh_4)_2$[**1-Re-MeCN**] (545 nm) < $(PPh_4)_2$[**1-Re-EtOH**] (548 nm). The emission quantum yield (Φ_{em}) and lifetime (τ_{em}) of the complexes were also dependent on the nature of the axial ligand. $(PPh_4)_2$[**1-Re-acetone**] (τ_{em} = 21 μs) and $(PPh_4)_2$[**1-Re-MeCN**] (τ_{em} = 2.0 μs) exhibited single-exponential emission decay profiles, while $(PPh_4)_2$[**1-Re-MeOH**] (τ_{em} = 0.41, 2.2, and 11 μs) and $(PPh_4)_2$[**1-Re-EtOH**] (τ_{em} = 5.5 and 18 μs) showed multiexponential decay profiles. These complicated emission decays observed for $(PPh_4)_2$[**1-Re-MeOH**] and $(PPh_4)_2$[**1-Re-EtOH**] may be partly due to evaporation of the solvent molecules in the solid state during emission lifetime measurements, as suggested by the thermogravimetric experiments, although the emission spectroscopy of the complexes was conducted in a MeOH or EtOH vapor atmosphere immediately after sampling the crystals from the relevant mother liquid solution. Interestingly, $(PPh_4)_2$[**1-Re-acetone**] showed intense emission (Φ_{em} = 0.34) compared with other complexes (Table 3). At the present stage of the investigation, the reason for the large Φ_{em} and long τ_{em} values of the acetone complex is unclear. The emission spectra of $(PPh_4)_2$[**1-Re-L**] (L = MeOH, EtOH, acetone, or MeCN) at 77 K are shown in Figure 3. The spectra exhibited vibronic structures, and the emission lifetimes were much longer than the relevant value at 296 K. The vibrational progressions observed for the complexes (ca. 1000 cm^{-1}) are in agreement with the $\nu_{Re\equiv N}$ stretching band frequencies commonly observed for nitridorhenium(V) complexes.[3b,c,e−g,19] These emission spectral and photophysical features are typical to those of the d^2 nitrido or oxo metal complexes showing

dx.doi.org/10.1021/ic202243d | Inorg. Chem. 2012, 51, 12065−12074

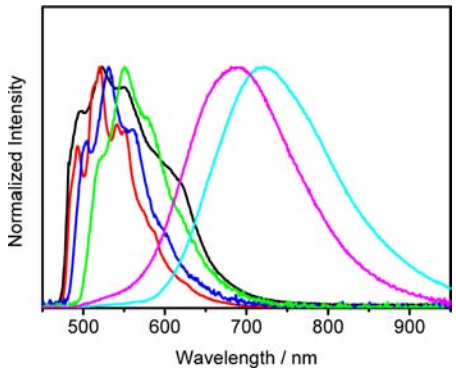

Figure 3. Emission spectra of $(PPh_4)_2$[**1-Re-MeOH**] (black), $(PPh_4)_2$[**1-Re-EtOH**] (red), $(PPh_4)_2$[**1-Re-acetone**] (blue), $(PPh_4)_2$[**1-Re-MeCN**] (lime green), $(PPh_4)_2$[**1-Re**] (cyan), and $(PPh_4)_2$[**1′-Re**] (magenta) in the solid state at 77 K.

$^3[(d_{xy})^1(d_{\pi^*})^1]$ emissive excited states.[2a−f,h,3,5a,e,19l,20,21] The σ-donating ability of the axial ligand influences the strength of the Re≡N bond. The $(d_{xy})^2 \rightarrow (d_{xy})^1(d_{\pi^*})^1$ absorption transition and emission from the $^3[(d_{xy})^1(d_{\pi^*})^1]$ excited state were shifted to the longer wavelengths with increasing π-donating and -accepting abilities of the axial ligand in $[ReN(dppe)_2X]^+$ (dppe = $Ph_2PCH_2CH_2PPh_2$; X = F, Cl, Br, I).[3f] Therefore, the electron-donating and -accepting abilities of the axial ligand may have an influence on the emission maximum wavelength in the present complexes and vapochromic luminescence spectral changes as described later. However, no correlation was found between the emission energy and the electron-donating and -accepting parameters of the solvent ligand, namely the donor and acceptor numbers and dielectric constant.

Among the six-coordinate rhenium complexes, $(PPh_4)_2$[**1-Re-MeOH**] and $(PPh_4)_2$[**1-Re-EtOH**] exhibited emission at 296 K in neat MeOH and EtOH solutions, respectively (Supporting Information, Table S1 and Figure S14). The Φ_{em} and τ_{em} values are significantly smaller and shorter, respectively, than the relevant values in the crystalline phase. The acetone and MeCN complexes were almost not emissive in acetone and MeCN, respectively. The weak photoluminescence of the complexes in the solutions is due to thermal deactivation through coordination/dissociation of the solvent molecule with the parent complex because the bond between the Re ion and the axial ligand is very weak and the axial site is labile.[11]

Figure 2 also shows the emission spectra of $(PPh_4)_2$[**1-Re**] and $(PPh_4)_2$[**1′-Re**] in the solid state at 296 K. The moderately long emission lifetimes of both $(PPh_4)_2$[**1-Re**] and $(PPh_4)_2$[**1′-Re**] (τ_{em} = 0.35−7.6 μs) indicate that the emission possesses a spin triplet character. The square-pyramidal five-coordinate $(PPh_4)_2$[**1′-Re**] complex in the crystalline phase at 296 K showed the emission maximum at 689 nm with a shoulder at ca. 550 nm. The full-width at half-maximum (fwhm) value of the emission band (5200 cm^{-1}) of $(PPh_4)_2$[**1′-Re**] is significantly larger than the values observed for the six-coordinate complexes (3180−3800 cm^{-1}). In the case of $(PPh_4)_2$[**1-Re**] at 296 K, two emission bands were observed at 569 and ca. 720 nm. At 77 K, the emission spectra of both $(PPh_4)_2$[**1′-Re**] and $(PPh_4)_2$[**1-Re**] are best characterized by the intense emission bands at around 700 nm with the very weak emission bands at around 550 nm, as shown in Figure 3. The vibronic structures of the emission spectra were not observed at 77 K for both five-coordinate complexes. The two emission bands at shorter (ca. 550−570 nm) and longer (ca. 700 nm) wavelengths may be ascribed to the emission from the square-pyramidal complex. The emission maximum wavelengths (λ_{em}) and the intensity ratio of the band at ca. 550 nm to that at ca. 700 nm were different for $(PPh_4)_2$[**1′-Re**] and $(PPh_4)_2$[**1-Re**]. This might be due to the difference in the microenvironments around the complex: crystal packing and the presence or absence of a noncoordinating solvent molecule(s) in the crystal lattice. In practice, the hydrogen bond between the O atom in the isopropyl alcohol ligand and the cyanide ligand [O1···N3 = 2.823(5) Å] participates in the $(PPh_4)_2$[**1′-Re**] crystal, as demonstrated by the X-ray structure of the complex. In $[MnN(CN)_4]^{2-}$ and $[MnN(CN)_5]^{3-}$, the electronic transition assignable to $(d_{xy})^2 \rightarrow (d_{xy})^1(d_{\pi^*})^1$ of $[MnN(CN)_4]^{2-}$ showed at higher energy than that of $[MnN(CN)_5]^{3-}$ because (i) the axial CN^- ligand acts as a π acceptor and stabilizes the d_{π^*} level and (ii) the Mn≡N distance is shortened by the lack of the sixth ligand.[18a] The emission maximum wavelengths for $[$**1′-Re**$]^{2-}$ and $[$**1-Re**$]^{2-}$ were longer than those of $[ReN(CN)_4L]^{2-}$ (L = MeOH, EtOH, acetone, or MeCN). This is a tendency opposite to the transition energy shift of $(d_{xy})^2 \rightarrow (d_{xy})^1(d_{\pi^*})^1$ in the five- and six-coordinate manganese(V) complexes. It is reported that the energy level of d_{z^2} is stabilized, while d_π is destabilized by decreasing the L−M−L (trans) angle of the four equatorial L ligands in the five-coordinate square-pyramidal complex, ML_5.[22] The density functional theory (DFT) calculations of $[CrN(CN)_5]^{3-}$ and $[CrN(CN)_4]^{2-}$ proposed that the HOMO is d_{xy} in both six- and five-coordinate complexes.[18b] On the other hand, LUMOs of the six- and five-coordinate chromium complexes are different from each other; the LUMO of the six-coordinate complex is d_{π^*} and that of the five-coordinate complex is an admixed d_{z^2}−p_z hybrid.[18b] The C−Re−C (trans) angles of the five-coordinate rhenium(V) complex are significantly smaller than the corresponding six-coordinate complexes, as described in Crystal Structures section. Therefore, the d_{z^2} level of the five-coordinate complex may be stabilized in energy compared with that of the six-coordinate complex. The significant differences of the emission spectral features for six- and five-coordinate rhenium(V) complexes in this study might be caused by the difference in the contributions of d_{z^2} to the LUMO between the six- and five-coordinate complexes.

Both the six- and five-coordinate technetium complexes, $(PPh_4)_2$[**1-Tc-MeOH**] and $(PPh_4)_2$[**1-Tc**], respectively, showed emission in the solid state at room temperature, as shown in Figure 4. These complexes are the first reported

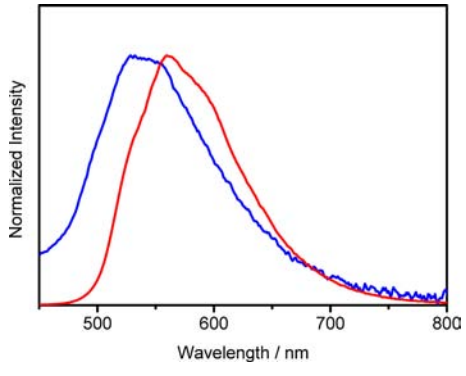

Figure 4. Emission spectra of $(PPh_4)_2$[**1-Tc-MeOH**] (red) and $(PPh_4)_2$[**1-Tc**] (blue) in the solid state at room temperature.

dx.doi.org/10.1021/ic202243d | *Inorg. Chem.* 2012, 51, 12065−12074

nitridotechnetium complexes showing photoluminescence. $(PPh_4)_2$[**1-Tc-MeOH**] exhibited an emission maximum at 559 nm with vibronic bands at 529 and 594 nm. The vibrational progressions (ca. 1000 cm^{-1}) agree with the $\nu_{Tc\equiv N}$ stretching frequency commonly observed in nitridotechnetium(V) complexes.[19c,f,m,o,23] The spectroscopic feature of the six-coordinate nitridotechnetium complex is similar to that of the rhenium analogues, although the detailed photophysical data such as Φ_{em} and τ_{em} of the technetium complex have not been obtained at the present stage of the investigation. The emission observed for $(PPh_4)_2$[**1-Tc-MeOH**] can be assigned as originating from the $^3[(d_{xy})^1(d_{\pi^*})^1]$ excited state. $(PPh_4)_2$[**1-Tc-MeOH**] was not emissive in MeOH at room temperature. The emission maximum wavelength of $(PPh_4)_2$[**1-Tc**] (528 nm) is shifted to shorter wavelength relative to that of $(PPh_4)_2$[**1-Tc-MeOH**] (559 nm). The spectrum shows the vibronic structures with the progression of ca. 1000 cm^{-1}, whose value corresponds to the $\nu_{Tc\equiv N}$ stretching frequency as discussed before.[19c,f,m,o,23] The blue shift of the emission maximum wavelength of the five-coordinate complex to the six-coordinate complex has the same tendency as that of the absorption maximum shift of the $(d_{xy})^2 \rightarrow (d_{xy})^1(d_{\pi^*})^1$ transition for the manganese complexes.[18a] Therefore, the emission from $(PPh_4)_2$[**1-Tc**] seems to have originated from the $^3[(d_{xy})^1(d_{\pi^*})^1]$ excited state.

Vapochromic Luminescence of Six-Coordinate Complexes. Vapochromic luminescence from the six-coordinate rhenium complexes upon exposure of the VOC (MeOH, EtOH, acetone, or MeCN) was investigated. Figures S16–S39 in the Supporting Information show the emission spectral changes of powdered $(PPh_4)_2$[**1-Re-L**] (L = MeOH, EtOH, acetone, or MeCN) by exposure of VOC vapor (MeOH, EtOH, acetone, or MeCN) under a N_2-gas atmosphere at room temperature, and the VOC vapor exposure time (t) dependences of the molar ratios of the residual solvent molecule/incorporated VOC in the solid state to the complex anion. The ratio of the complex anion to the residual solvent molecule or incorporated VOC in the solid state was evaluated based on the integrated intensity ratio of the proton signal of the $(PPh_4)^+$ ion to those of the solvent molecule and VOC in the ^1H NMR spectrum in $CDCl_3$. In the case of the reaction of $(PPh_4)_2$[**1-Re-MeOH**] with acetone vapor, as an example, the emission spectrum was shifted to longer wavelength during acetone vapor exposure and converted to that of the acetone-coordinating complex at t > 300 min (Supporting Information, Figure S18). In the solid state, the amount of MeOH in $(PPh_4)_2$[**1-Re-MeOH**] gradually decreased with t, while acetone increased with t (Supporting Information, Figure S19). These data indicate that one acetone molecule per complex anion can be incorporated in the solid state upon exposure of acetone vapor, leading to switching of the emission spectrum of the acetone complex. This demonstrates that the incorporated acetone coordinates at the axial site of the complex anion. When the powdered acetone-coordinating complex was exposed to MeOH vapor in a N_2-gas atmosphere at room temperature, the emission spectrum varied to that of the MeOH complex after 17 min. Figure S28 in the Supporting Information shows the time profile of the emission spectrum of $(PPh_4)_2$[**1-Re-acetone**] under exposure of MeOH. Figure S29 in the Supporting Information exhibits the time profiles of the molar ratios of acetone and MeOH to the complex anion, determined by ^1H NMR spectroscopy in $CDCl_3$. The ^1H NMR spectra revealed that acetone disappeared at t > 17 min and four MeOH molecules per complex anion were incorporated in the solid. Therefore, vapochromic luminescence between the MeOH- and acetone-coordinating complexes is reversible. Scheme 1 summarizes the results of conversion of photoluminescence between the six-coordinate complexes. The reversible conversions between these complexes were confirmed experimentally except for that between the acetone and MeCN complexes. In the reversible reactions, four MeOH, three EtOH, one acetone, and one MeCN molecules per complex anion were incorporated into the relevant solid complex upon exposure of each VOC vapor, giving rise to the emission spectrum of the complex coordinated to each VOC molecule, while the solvent molecules in the starting materials had almost disappeared. In the case of the reaction of $(PPh_4)_2$[**1-Re-acetone**] with MeCN vapor, the emission spectrum did not show complete conversion to $(PPh_4)_2$[**1-Re-MeCN**] and the acetone partially remained in the solid even after 180 min of exposure to MeCN vapor (Supporting Information, Figures S32 and S33). In the reverse reaction, the emission spectrum varied to that of $(PPh_4)_2$[**1-Re-acetone**] by exposure of acetone vapor to $(PPh_4)_2$[**1-Re-MeCN**], while the amount of the residual MeCN molecule was 0.38 per complex anion after 500 min of exposure of acetone vapor (Supporting Information, Figures S38 and S39). The Φ_{em} value of $(PPh_4)_2$[**1-Re-acetone**] is much higher than that of $(PPh_4)_2$[**1-Re-MeCN**]. Therefore, the emission spectral band shape is characterized as that of the partially remaining acetone complex in the reaction of $(PPh_4)_2$[**1-Re-acetone**] with MeCN vapor, and the spectrum from the reaction of $(PPh_4)_2$[**1-Re-MeCN**] with acetone vapor displayed the acetone complex even after partial substitution of MeCN by acetone.

Scheme 1. Interconversion Reactions of the Six- and Five-Coordinate Nitridorhenium(V) Complexes in the Solid State at Room Temperature[a]

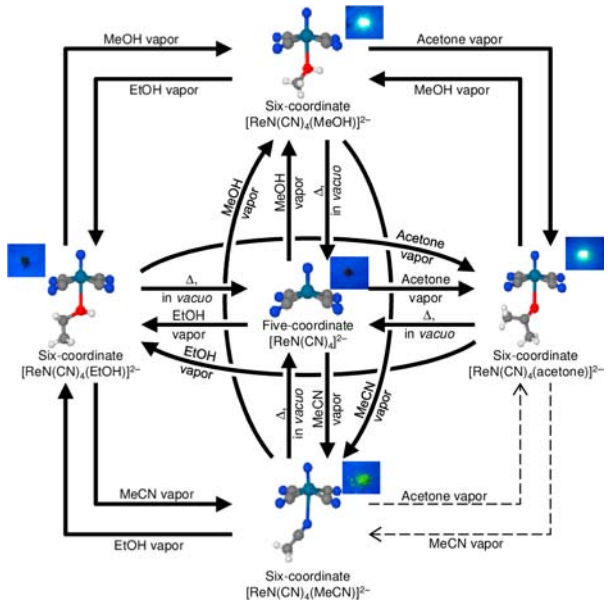

[a]Bold and dashed arrows show reversible and incomplete reactions, respectively.

The vapochromic luminescence behavior of the technetium complex was also investigated for the reaction of $(PPh_4)_2$[**1-Tc-MeOH**] with acetone vapor in the solid state under a N_2-gas atmosphere at room temperature. Surprisingly, the emission

dx.doi.org/10.1021/ic202243d | Inorg. Chem. 2012, 51, 12065–12074

spectrum of $(PPh_4)_2$[**1-Tc-MeOH**] changed to that of the five-coordinate $(PPh_4)_2$[**1-Tc**] by exposure to acetone vapor (Supporting Information, Figure S40). The IR spectrum after exposure of acetone vapor for several hours was in good agreement with the five-coordinate complex (Supporting Information, Figure S41). This suggests that the coordinating MeOH molecule in $(PPh_4)_2$[**1-Tc-MeOH**] was eliminated under an acetone vapor atmosphere, but acetone was not incorporated and did not coordinate at the axial site in the technetium complex.

Vapochromic Luminescence between Five- and Six-Coordinate Complexes. Vapochromic luminescence between the bistable five- and six-coordinate complexes with the VOCs (MeOH, EtOH, acetone, or MeCN) was investigated. The emission maximum wavelength of $(PPh_4)_2$[**1-Re**] changed to that of the six-coordinate complex bearing a VOC molecule at the axial site, when five-coordinate $(PPh_4)_2$[**1-Re**] in the solid state was exposed to VOC vapor in a N_2-gas atmosphere at room temperature. Figures S42−S49 in the Supporting Information show emission spectral changes upon exposure of VOCs to $(PPh_4)_2$[**1-Re**] in the solid state at room temperature, as well as the time profiles of the molar ratios of the VOCs incorporated into the complex anion. The ratio of the incorporated VOC to each complex anion was determined based on the integrated intensity ratio of the proton signal from the $(PPh_4)^+$ ion to that of the VOC in the ^1H NMR spectra in $CDCl_3$. These results demonstrate that coordination of a VOC at the axial site of each five-coordinate compound gives rise to the formation of the six-coordinate complex, where approximately four MeOH, three EtOH, one acetone, or one MeCN molecule(s) per complex anion are (is) incorporated in the solid. When the complexes after exposure of the given VOC vapor to $(PPh_4)_2$[**1-Re**] were left in vacuo at 95 °C for 4 h, the emission spectra of the complexes returned to that of the original $(PPh_4)_2$[**1-Re**]. These behaviors suggest reversible coordination and elimination of the VOCs at the axial position of $[ReN(CN)_4]^{2-}$, demonstrating luminescent vapochromism between the five- and six-coordinate complexes. Scheme 1 summarizes the results of the interconversion reactions between the five- and six-coordinate complexes upon VOC vapor exposure.

The incorporation of MeOH into the technetium complex in the solid state upon MeOH vapor exposure was also investigated by emission and IR spectroscopies. Upon exposure of $(PPh_4)_2$[**1-Tc**] to MeOH vapor for 10 min, the emission spectrum changed to that of $[$**1-Tc-MeOH**$]^{2-}$ and the new IR bands originating from MeOH appeared at 1038 and 1076 cm^{-1} accompanied by the appearance of C≡N stretching bands similar to that observed for $(PPh_4)_2$[**1-Tc-MeOH**] (Supporting Information, Figure S6). The coordinating MeOH molecule can be removed by evacuation of the complex in vacuo at 95 °C for 4 h to regenerate $(PPh_4)_2$[**1-Tc**], indicating that coordination/elimination of MeOH between the six- and five-coordinate technetium complexes is reversible. In contrast, the emission and IR spectral band shapes of $(PPh_4)_2$[**1-Tc**] remained unchanged even upon exposure of acetone vapor for 42 min (Supporting Information, Figures S40 and S50). These results suggest that the stronger trans influence/trans effect of the Tc≡N bond compared to that of the Re≡N bond prevents coordination of acetone at the axial site in the technetium complex.

CONCLUSION

The tetracyanidonitridorhenium(V) and -technetium(V) complexes, $[MN(CN)_4L]^{2-}$ (M = Re, L = MeOH, EtOH, acetone, or MeCN; M = Tc, L = MeOH) and $[MN(CN)_4L]^{2-}$ (M = Re or Tc), were synthesized and characterized by X-ray crystallographic analysis and IR/UV−vis/emission spectroscopies. Results demonstrate that the tetracyanidonitridorhenium(V) and -technetium(V) complexes were bistable between the five-coordinate square-pyramidal and six-coordinate octahedral coordination environments. All of the five-coordinate square-pyramidal and six-coordinate octahedral complexes showed photoluminescence in the solid state at room temperature. The photoemission of six-coordinate complexes originated from the $^3[(d_{xy})^1(d_{\pi^*})^1]$ excited state revealed from absorption/emission spectroscopies. The emission spectra and photophysical data of the five-coordinate $[ReN(CN)_4]^{2-}$ were significantly different from those of the relevant six-coordinate complexes. This may be caused by the difference in the contribution of d_{z^2} to the LUMO between the six- and five-coordinate complexes. We found unique reversible coordination and elimination of a VOC at the axial site of the complex in the solid state that gave rise to changes in the emission maximum wavelength, demonstrating photoluminescence switching and sensing of VOC by the present rhenium(V) and technetium(V) complexes at room temperature.

ASSOCIATED CONTENT

Supporting Information

Crystallographic data in CIF format, a table of spectroscopic and photophysical data in the solution, figures of thermogravimetric and differential thermal analysis curves, IR spectra, UV−vis spectra, emission spectral changes by exposure of VOC vapor, and molar ratios of residual VOC/incorporated VOC in the solid to the complex anion against the exposure time of VOC. This material is available free of charge via the Internet at http://pubs.acs.org.

AUTHOR INFORMATION

Corresponding Author

*E-mail: tyoshi@rirc.osaka-u.ac.jp. Tel: +81-6-6879-8821. Fax: +81-6-6879-8825.

Notes

The authors declare no competing financial interest.

REFERENCES

(1) Kirgan, R. A.; Sullivan, B. P.; Rillema, D. P. *Top. Curr. Chem.* **2007**, *281*, 45−100.

(2) (a) Winkler, J. R.; Gray, H. B. *J. Am. Chem. Soc.* **1983**, *105*, 1373−1374. (b) Winkler, J. R.; Gray, H. B. *Inorg. Chem.* **1985**, *24*, 346−355. (c) Newsham, M. D.; Giannelis, E. P.; Pinnavaia, T. J.; Nocera, D. G. *J. Am. Chem. Soc.* **1988**, *110*, 3885−3891. (d) Thorp, H. H.; Van Houten, J.; Gray, H. B. *Inorg. Chem.* **1989**, *28*, 889−892. (e) Savoie, C.; Reber, C. *Coord. Chem. Rev.* **1998**, *171*, 387−398. (f) Savoie, C.; Reber, C. *J. Am. Chem. Soc.* **2000**, *122*, 844−852. (g) Grey, J. K.; Triest, M.; Butler, I. S.; Reber, C. *J. Phys. Chem. A* **2001**, *105*, 6269−6272. (h) Grey, J. K.; Butler, I. S.; Reber, C. *J. Am. Chem. Soc.* **2002**, *124*, 11699−11708.

(3) (a) Neyhart, G. A.; Bakir, M.; Boaz, J.; Vining, W. J.; Sullivan, B. P. *Coord. Chem. Rev.* **1991**, *111*, 27−32. (b) Neyhart, G. A.; Seward, K. J.; Boaz, J.; Sullivan, B. P. *Inorg. Chem.* **1991**, *30*, 4486−4488. (c) Yam, V. W. W.; Tam, K. K.; Cheng, M. C.; Peng, S. M.; Wang, Y. *J. Chem. Soc., Dalton Trans.* **1992**, 1717−1723. (d) Yam, V. W. W.; Tam, K. K.; Lai, T. F. *J. Chem. Soc., Dalton Trans.* **1993**, 651−652. (e) Yam, V. W. W.; Tam, K. K. *J. Chem. Soc., Dalton Trans.* **1994**, 391−392. (f) Yam,

V. W.-W.; Tam, K.-K.; Cheung, K.-K. *J. Chem. Soc., Dalton Trans.* **1996**, 1125−1132. (g) Yam, V. W.-W.; Pui, Y. L.; Man-Chung Wong, K.; Cheung, K. K. *Inorg. Chim. Acta* **2000**, *300*−*302*, 721−732. (h) Bailey, S. E.; Eikey, R. A.; Abu-Omar, M. M.; Zink, J. I. *Inorg. Chem.* **2002**, *41*, 1755−1760.

(4) (a) Yoshimura, T.; Matsuda, A.; Ito, Y.; Ishizaka, S.; Shinoda, S.; Tsukube, H.; Kitamura, N.; Shinohara, A. *Inorg. Chem.* **2010**, *49*, 3473−3481. (b) Yoshimura, T.; Suo, C.; Tsuge, K.; Ishizaka, S.; Nozaki, K.; Sasaki, Y.; Kitamura, N.; Shinohara, A. *Inorg. Chem.* **2010**, *49*, 531−540.

(5) (a) Del Negro, A. S.; Wang, Z.; Seliskar, C. J.; Heineman, W. R.; Sullivan, B. P.; Hightower, S. E.; Hubler, T. L.; Bryan, S. A. *J. Am. Chem. Soc.* **2005**, *127*, 14978−14979. (b) Kurz, P.; Probst, B.; Spingler, B.; Alberto, R. *Eur. J. Inorg. Chem.* **2006**, 2966−2974. (c) Del Negro, A. S.; Seliskar, C. J.; Heineman, W. R.; Hightower, S. E.; Bryan, S. A.; Sullivan, B. P. *J. Am. Chem. Soc.* **2006**, *128*, 16494−16495. (d) Briggs, B. N.; McMillin, D. R.; Todorova, T. K.; Gagliardi, L.; Poineau, F.; Czerwinski, K. R.; Sattelberger, A. P. *Dalton Trans.* **2010**, *39*, 11322−11324. (e) Chatterjee, S.; Del Negro, A. S.; Wang, Z.; Edwards, M. K.; Skomurski, F. N.; Hightower, S. E.; Krause, J. A.; Twamley, B.; Sullivan, B. P.; Reber, C.; Heineman, W. R.; Seliskar, C. J.; Bryan, S. A. *Inorg. Chem.* **2011**, *50*, 5815−5823.

(6) (a) Mansour, M. A.; Connick, W. B.; Lachicotte, R. J.; Gysling, H. J.; Eisenberg, R. *J. Am. Chem. Soc.* **1998**, *120*, 1329−1330. (b) Drew, S. M.; Janzen, D. E.; Buss, C. E.; MacEwan, D. I.; Dublin, K. M.; Mann, K. R. *J. Am. Chem. Soc.* **2001**, *123*, 8414−8415. (c) Buss, C. E.; Mann, K. R. *J. Am. Chem. Soc.* **2002**, *124*, 1031−1039. (d) Kato, M.; Omura, A.; Toshikawa, A.; Kishi, S.; Sugimoto, Y. *Angew. Chem., Int. Ed.* **2002**, *41*, 3183−3185. (e) Lu, W.; Chan, M. C. W.; Zhu, N.; Che, C.-M.; He, Z.; Wong, K.-y. *Chem.—Eur. J.* **2003**, *9*, 6155−6166. (f) White-Morris, R. L.; Olmstead, M. M.; Balch, A. L. *J. Am. Chem. Soc.* **2003**, *125*, 1033−1040. (g) Grove, L. J.; Rennekamp, J. M.; Jude, H.; Connick, W. B. *J. Am. Chem. Soc.* **2004**, *126*, 1594−1595. (h) Wadas, T. J.; Wang, Q.-M.; Kim, Y.-J.; Flaschenreim, C.; Blanton, T. N.; Eisenberg, R. *J. Am. Chem. Soc.* **2004**, *126*, 16841−16849. (i) Kato, M. *Bull. Chem. Soc. Jpn.* **2007**, *80*, 287−294. (j) Du, P.; Schneider, J.; Brennessel, W. W.; Eisenberg, R. *Inorg. Chem.* **2008**, *47*, 69−77. (k) Fornies, J.; Fuertes, S.; Lopez, J. A.; Martin, A.; Sicilia, V. *Inorg. Chem.* **2008**, *47*, 7166−7176. (l) Grove, L. J.; Oliver, A. G.; Krause, J. A.; Connick, W. B. *Inorg. Chem.* **2008**, *47*, 1408−1410. (m) Muro, M. L.; Daws, C. A.; Castellano, F. N. *Chem. Commun.* **2008**, 6134−6136. (n) Ni, J.; Wu, Y.-H.; Zhang, X.; Li, B.; Zhang, L.-Y.; Chen, Z.-N. *Inorg. Chem.* **2009**, *48*, 10202−10210. (o) Ni, J.; Zhang, L.-Y.; Wen, H.-M.; Chen, Z.-N. *Chem. Commun.* **2009**, 3801−3803. (p) Field, J. S.; Grimmer, C. D.; Munro, O. Q.; Waldron, B. P. *Dalton Trans.* **2010**, *39*, 1558−1567. (q) Du, P. *Inorg. Chim. Acta* **2010**, *363*, 1355−1358. (r) Strasser, C. E.; Catalano, V. J. *J. Am. Chem. Soc.* **2010**, *132*, 10009−10011. (s) Hudson, Z. M.; Sun, C.; Harris, K. J.; Lucier, B. E. G.; Schurko, R. W.; Wang, S. *Inorg. Chem.* **2011**, *50*, 3447−3457. (t) Lim, S. H.; Olmstead, M. M.; Balch, A. L. *J. Am. Chem. Soc.* **2011**, *133*, 10229−10238. (u) Ni, J.; Zhang, X.; Wu, Y.-H.; Zhang, L.-Y.; Chen, Z.-N. *Chem.—Eur. J.* **2011**, *17*, 1171−1183.

(7) (a) Cariati, E.; Bu, X.; Ford, P. C. *Chem. Mater.* **2000**, *12*, 3385−3391. (b) Osawa, M.; Kawata, I.; Igawa, S.; Hoshino, M.; Fukunaga, T.; Hashizume, D. *Chem.—Eur. J.* **2010**, *16*, 12114−12126.

(8) (a) Daws, C. A.; Exstrom, C. L.; Sowa, J. R., Jr.; Mann, K. R. *Chem. Mater.* **1997**, *9*, 363−368. (b) Lu, W.; Chan, M. C. W.; Cheung, K.-K.; Che, C.-M. *Organometallics* **2001**, *20*, 2477−2486. (c) Pang, J.; Marcotte, E. J. P.; Seward, C.; Brown, R. S.; Wang, S. *Angew. Chem., Int. Ed.* **2001**, *40*, 4042−4045. (d) Das, S.; Bharadwaj, P. K. *Inorg. Chem.* **2006**, *45*, 5257−5259. (e) Kui, S. C. F.; Chui, S. S.-Y.; Che, C.-M.; Zhu, N. *J. Am. Chem. Soc.* **2006**, *128*, 8297−8309. (f) Pattacini, R.; Giansante, C.; Ceroni, P.; Maestri, M.; Braunstein, P. *Chem.—Eur. J.* **2007**, *13*, 10117−10128. (g) Liu, Z.; Bian, Z.; Bian, J.; Li, Z.; Nie, D.; Huang, C. *Inorg. Chem.* **2008**, *47*, 8025−8030. (h) McGee, K. A.; Marquardt, B. J.; Mann, K. R. *Inorg. Chem.* **2008**, *47*, 9143−9145. (i) Abe, T.; Suzuki, T.; Shinozaki, K. *Inorg. Chem.* **2010**, *49*, 1794−1800. (j) Rawashdeh-Omary, M. A.; Rashdan, M. D.; Dharanipathi, S.; Elbjeirami, O.; Ramesh, P.; Dias, H. V. R. *Chem. Commun.* **2011**, *47*, 1160−1162.

(9) (a) Nastasi, F.; Puntoriero, F.; Palmeri, N.; Cavallaro, S.; Campagna, S.; Lanza, S. *Chem. Commun.* **2007**, 4740−4742. (b) Li, K.; Chen, Y.; Lu, W.; Zhu, N.; Che, C.-M. *Chem.—Eur. J.* **2011**, *17*, 4109−4112.

(10) (a) Fernandez, E. J.; Lopez-de-Luzuriaga, J. M.; Monge, M.; Olmos, M. E.; Perez, J.; Laguna, A.; Mohamed, A. A.; Fackler, J. P., Jr. *J. Am. Chem. Soc.* **2003**, *125*, 2022−2023. (b) Lefebvre, J.; Batchelor, R. J.; Leznoff, D. B. *J. Am. Chem. Soc.* **2004**, *126*, 16117−16125. (c) Fernandez, E. J.; Lopez-de-Luzuriaga, J. M.; Monge, M.; Olmos, M. E.; Puelles, R. C.; Laguna, A.; Mohamed, A. A.; Fackler, J. P., Jr. *Inorg. Chem.* **2008**, *47*, 8069−8076. (d) Laguna, A.; Lasanta, T.; Lopez-de-Luzuriaga, J. M.; Monge, M.; Naumov, P.; Olmos, M. E. *J. Am. Chem. Soc.* **2010**, *132*, 456−457.

(11) (a) Schwochau, K. *Technetium: Chemistry and Radiopharmaceutical Applications*; Wiley-VCH: Weinheim, Germany, 2000. (b) Abram, U. *Compr. Coord. Chem. II* **2004**, *5*, 271−402. (c) Alberto, R. *Compr. Coord. Chem. II* **2004**, *5*, 127−270. (d) Baldas, J. *Adv. Inorg. Chem.* **1994**, *41*, 1−123.

(12) Oetliker, U.; Savoie, C.; Stanislas, S.; Reber, C.; Connac, F.; Beauchamp, A. L.; Loiseau, F.; Dartiguenave, M. *Chem. Commun.* **1998**, 657−658.

(13) (a) Baldas, J.; Boas, J. F.; Bonnyman, J.; Williams, G. A. *J. Chem. Soc., Dalton Trans.* **1984**, 2395−2400. (b) Baldas, J.; Colmanet, S. F.; Williams, G. A. *Inorg. Chim. Acta* **1991**, *179*, 189−194.

(14) Johnson, N. P. *J. Chem. Soc. A* **1969**, 1843−1845.

(15) *TEXSAN*; Molecular Structure Corp.: The Woodlands, TX, 1985 and 1992.

(16) Baldas, J.; Boas, J. F.; Colmanet, S. F.; Mackay, M. F. *Inorg. Chim. Acta* **1990**, *170*, 233−239.

(17) (a) Purcell, W.; Potgieter, I. M.; Damoense, L. J.; Leipoldt, J. G. *Transition Met. Chem.* **1992**, *17*, 387−389. (b) Britten, J. F.; Lock, C. J. L.; Wei, Y. *Acta Crystallogr., Sect. C* **1993**, *C49*, 1277−1280. (c) Mtshali, T. N.; Purcell, W.; Visser, H. G. *Acta Crystallogr., Sect. E* **2007**, *E63*, m80−m82.

(18) (a) Bendix, J.; Meyer, K.; Weyhermueller, T.; Bill, E.; Metzler-Nolte, N.; Wieghardt, K. *Inorg. Chem.* **1998**, *37*, 1767−1775. (b) Bendix, J.; Deeth, R. J.; Weyhermüller, T.; Bill, E.; Wieghardt, K. *Inorg. Chem.* **2000**, *39*, 930−938. (c) van der Westhuizen, H. J.; Meijboom, R.; Schutte, M.; Roodt, A. *Inorg. Chem.* **2010**, *49*, 9599−9608.

(19) (a) Chatt, J.; Garforth, J. D.; Johnson, N. P.; Rowe, G. A. *J. Chem. Soc.* **1964**, 1012−1020. (b) Johnson, N. P. *J. Inorg. Nucl. Chem.* **1973**, *35*, 3141−3144. (c) Abram, U.; Spies, H.; Goerner, W.; Kirmse, R.; Stach, J. *Inorg. Chim. Acta* **1985**, *109*, L9−L11. (d) Mrwa, A.; Giegengack, H.; Starke, M. *Cryst. Res. Technol.* **1988**, *23*, 773−778. (e) Purcell, W.; Damoense, L. J.; Leipoldt, J. G. *Inorg. Chim. Acta* **1992**, *195*, 217−220. (f) Cros, G.; Belhadj, T. H.; de, M. D.; Gleizes, A.; Coulais, Y.; Guiraud, R.; Bellande, E.; Pasqualini, R. *Inorg. Chim. Acta* **1994**, *227*, 25−31. (g) Sievertsen, S.; Homborg, H. *Z. Anorg. Allg. Chem.* **1994**, *620*, 1439−1442. (h) Ziener, U.; Hanack, M. *Chem. Ber.* **1994**, *127*, 1681−1685. (i) Ziener, U.; Duerr, K.; Hanack, M. *Synth. Met.* **1995**, *71*, 2285−2286. (j) Ritter, S.; Abram, U. *Z. Anorg. Allg. Chem.* **1996**, *622*, 965−973. (k) Demaimay, F.; Roucoux, A.; Noiret, N.; Patin, H. *J. Organomet. Chem.* **1999**, *575*, 145−148. (l) Dablemont, C.; Hamaker, C. G.; Thouvenot, R.; Sojka, Z.; Che, M.; Maatta, E. A.; Proust, A. *Chem.—Eur. J.* **2006**, *12*, 9150−9160. (m) Bolzati, C.; Cavazza-Ceccato, M.; Agostini, S.; Tisato, F.; Bandoli, G. *Inorg. Chem.* **2008**, *47*, 11972−11983. (n) Lopez-Torres, E.; Abram, U. *Inorg. Chem.* **2008**, *47*, 2890−2896. (o) Schroer, J.; Abram, U. *Polyhedron* **2011**, *30*, 2157−2161.

(20) (a) Grey, J. K.; Marguerit, M.; Butler, I. S.; Reber, C. *Chem. Phys. Lett.* **2002**, *366*, 361−367. (b) Isovitsch, R. A.; Beadle, A. S.; Fronczek, F. R.; Maverick, A. W. *Inorg. Chem.* **1998**, *37*, 4258−4264. (c) Lanthier, E.; Bendix, J.; Reber, C. *Dalton Trans.* **2010**, *39*, 3695−3705. (d) Che, C.-M.; Lam, M. H.-W.; Mak, T. C. W. *J. Chem. Soc., Chem. Commun.* **1989**, 1529−1531. (e) Che, C.-M.; Lau, T.-C.; Lam, H.-W.; Poon, C.-K. *J. Chem. Soc., Chem. Commun.* **1989**, 114−116.

(f) Che, C. M.; Wong, K. Y.; Lam, H. W.; Chin, K. F.; Zhou, Z. Y.; Mak, T. C. W. *J. Chem. Soc., Dalton Trans.* **1993**, 857−856. (g) Lam, H.-W.; Chin, K.-F.; Che, C.-M.; Wang, R.-J.; Mak, T. C. W. *Inorg. Chim. Acta* **1993**, *204*, 133−137. (h) Chin, K.-F.; Cheung, K.-K.; Yip, H.-K.; Mak, T. C. W.; Che, C. M. *J. Chem. Soc., Dalton Trans.* **1995**, 657−663. (i) Wong, T.-W.; Lau, T.-C.; Wong, W.-T. *Inorg. Chem.* **1999**, *38*, 6181−6186. (j) Lai, S.-W.; Lau, T.-C.; Fung, W. K. M.; Zhu, N.; Che, C.-M. *Organometallics* **2003**, *22*, 315−320. (k) Zhang, Y.-H.; Xia, B.-H.; Pan, Q.-J.; Zhang, H.-X. *J. Chem. Phys.* **2006**, *124*, 144309/144301−144309/144308.

(21) The Re≡N stretching band could not be assigned because the Raman bands of $(PPh_4)^+$ overlapped with that of the Re≡N stretching band. The resonance Raman spectra of the rhenium complexes could not be obtained because of interference by photoluminescence of the complexes.

(22) Rossi, A. R.; Hoffmann, R. *Inorg. Chem.* **1975**, *14*, 365−374.

(23) (a) Baldas, J.; Bonnyman, J.; Williams, G. A. *Inorg. Chem.* **1986**, *25*, 150−153. (b) Baldas, J.; Bonnyman, J. *Inorg. Chim. Acta* **1988**, *141*, 153−154. (c) De, V. N.; Costello, C. E.; Jones, A. G.; Davison, A. *Inorg. Chem.* **1990**, *29*, 1348−1352. (d) Bolzati, C.; Boschi, A.; Uccelli, L.; Tisato, F.; Refosco, F.; Cagnolini, A.; Duatti, A.; Prakash, S.; Bandoli, G.; Vittadini, A. *J. Am. Chem. Soc.* **2002**, *124*, 11468−11479.